Iron-enhanced coagulation is attenuated by chelation: a thrombelastographic and ultrastructural analysis

Vance G. Nielsen[a] and Etheresia Pretorius[b]

Department of Anesthesiology, The University of Arizona College of Medicine, Tucson, Arizona, USA and [b]Department of Physiology, Faculty of Health Sciences, University of Pretoria, Arcadia, South Africa

Correspondence to Vance G. Nielsen, MD., Department of Anesthesiology, The University of Arizona College of Medicine, P.O. Box 245114, 1501 North Campbell Avenue, Tucson, Arizona 85724-5114, USA
Tel: +1 520 626-7195; fax: +1 520 626-6943; e-mail: vgnielsen333@gmail.com

Increased circulating ferritin and free iron have been found in a variety of disease states associated with thrombophilia. When blood or plasma is exposed to iron addition, characteristic changes in thrombus formation are observed by scanning electron microscopy, which include fusion of fibrin polymers, matting, and even sheeting of fibrin.
A primary mechanism posited to explain iron-mediated hypercoagulability is hydroxyl radical formation and modification of fibrinogen; however, iron has also been demonstrated to bind to fibrinogen. We have recently demonstrated that iron enhances coagulation, manifested as a decrease in the time of onset of coagulation. Using clinically encountered concentrations of iron created by addition of $FeCl_3$ to human plasma, we demonstrated that iron-mediated changes in reaction time determined by thrombelastography or changes in thrombus ultrastructure were significantly, but not completely, reversed by iron chelation with deferoxamine. Thus, reversible iron binding to fibrinogen mechanistically explains a significant portion of coagulation kinetic and ultrastructural hypercoagulability. Further investigation is needed to determine whether residual iron binding or other iron-mediated effects is responsible for hypercoagulability observed after chelation.

Keywords: coagulation, electron microscopy, iron, thrombelastography

Introduction

As has been recently reviewed [1], increased circulating ferritin and free iron have been found in a variety of disease states associated with thrombophilia. When blood or plasma is exposed to iron addition, characteristic changes in thrombus formation are observed, which include fusion of fibrin polymers, matting, and even sheeting of fibrin [1–6]. This scanning electron micrographic (SEM) signature has also been documented in thrombi obtained from patients with diseases involving chronic iron overload [1,2,7,8]. It has been posited that iron-derived hydroxyl radicals interact with fibrinogen, resulting in hypercoagulation and hypofibrinolysis [1,3,9,10]. Of interest, exposing plasma to iron chelators such as deferoxamine or antioxidants significantly attenuated ultrastructural change in clots exposed to exogenous iron [11]. Further, plasma obtained from patients with hemochromatosis or chronic hyperferritinemia demonstrated a SEM signature similar to that of iron exposure that was attenuated by deferoxamine [12]. In sum, although not directly demonstrated, it appeared that iron–fibrinogen interactions resulted in characteristic clot ultrastructure similar to that of diseases with chronic iron overload and thrombophilia.

On the contrary, the concept that iron-modified fibrinogen via hydroxyl radical exposure is not supported by the observation that the procoagulant properties of fibrinogen are compromised by essentially all radical species tested by other investigators [13,14]. Indeed, given the concentration of antioxidants present in plasma (>1600 μmol/l) [15], it is unlikely that the addition of 6–30 μmol/l ferric chloride could generate hydroxyl radicals that exclusively affect fibrinogen. Instead, it appeared that iron directly bound to fibrinogen in a recent study [16]. Thus, it seems more plausible that iron–fibrinogen binding and potential fibrinogen conformational change may enhance coagulation. Iron-mediated phenomenon may be similar to that observed with enhancement of fibrinogen after carbon monoxide exposure [17]. Thus, modulation of the effects of iron on coagulation with chelation would speak strongly for an important role of iron-binding rather than only radical damage.

Although the precise molecular mechanism by which iron affects fibrinogen remained to be elucidated, we recently published an investigation of the effects of a small concentration (10 μmol/l) of ferric chloride on coagulation and fibrinolysis [18]. We found that the thrombelastographic, kinetic *sine quo non* of iron was a decrease in the onset time of coagulation and an increase in the velocity of thrombus growth [18]. The SEM signature of thrombi exposed to this small concentration of iron [18] demonstrated the typical changes previously mentioned [1–6]. Thus, the purpose of this study was to evaluate the effects of deferoxamine-mediated chelation on iron-exposed plasma with thrombelastographic and SEM-based analyses.

Methods

Thrombelastograph-based analyses

All thrombelastograph-based experiments were performed at the University of Arizona. Frozen, citrate anticoagulated normal pooled plasma was obtained from a commercial vendor (George King Bio-Medical, Overland Park, Kansas, USA) for use in subsequently described experimentation. With regard to chemicals utilized, ferric chloride ($FeCl_3$, 99.9% pure) and calcium-free phosphate-buffered saline (PBS) were obtained from a commercial vendor (Sigma-Aldrich, Saint Louis, Missouri, USA). Deferoxamine was obtained from a commercial vendor (Cayman Chemical Company, Ann Arbor, Michigan, USA).

First, a concentration–response relationship of iron concentration and reaction time (R, defined as 2 mm clot strength; this is also known as clotting time in thromboelastometric analyses) was determined. The rationale for using R time was that it is the first indication of the onset of coagulation, is used in both thrombelastographic and thromboelastometric systems, and is anticipated to quickly and easily detect iron-mediated enhancement of coagulation based on our previous work under review. This concentration–response relationship was generated with a ROTEM *delta* hemostasis system (Tem Innovations GmbH, Munich, Germany) generously provided by the manufacturer. All disposable cups/pins and reagents were also provided by Tem Innovations. Plasma was rapidly thawed at 37°C on the day of experimentation. Separate aliquots of plasma were exposed to 1% v/v additions of ferric chloride dissolved in PBS that resulted in final concentrations of 0-10 μmol/l ($n = 5–6$ replicates per concentration). After 3 min or more of incubation at room temperature, 320 μl of these iron-exposed plasmas was subsequently placed in a disposable cup, with subsequent addition of 20 μl of 200 mmol/l $CaCl_2$. The complete sample was mixed by pipette once, and the reaction commenced at 37°C. The R values were subsequently recorded.

The second series of experiments examined the role of time on chelation of iron from plasma and consequent changes in R. First, plasma that was rapidly thawed at 37°C on the day of experimentation was exposed to either a 1% v/v addition of PBS or $FeCl_3$ (10 μmol/l final concentration) for 3 min. Then, 336 μl of either plasma mixture was placed in a disposable cup in a computer-controlled thrombelastograph hemostasis system (Model 5000; Haemoscope Corp., Niles, Illinois, USA). An addition of 3.6 μl deferoxamine in dH_2O (0 or 1 mmol/l final concentration) was added to the plasma mixture, mixed with the disposable pin, and allowed to incubate for 3 min at 37°C. Thus, there were four conditions: no deferoxamine, no $FeCl_3$, (Control), deferoxamine, no $FeCl_3$ (Deferoxamine); no deferoxamine, $FeCl_3$ ($FeCl_3$); and finally, $FeCl_3$ followed by deferoxamine ($FeCl_3$ + Deferoxamine). Thereafter, 20 μl of 200 mmol/l $CaCl_2$ was added as the last step to initiate clotting. Data were collected at 37°C for until R was recorded. In the next set of this experimental series, an identical addition of PBS or $FeCl_3$ to plasma was performed with a 3-min incubation, followed by a 1% v/v of deferoxamine (0 or 1 mmol/l final concentration), with this plasma kept in a sealed tube at room temperature for approximately 40 min. An aliquot of 340 μl of each of the four conditions was placed into thrombelastographic cups and 20 μl of 200 mmol/l $CaCl_2$ was added to initiate clotting. Data were collected at 37°C until R was recorded. There were six replicates per condition for all conditions in these series of experiments. As R values varied between experiments, and a fixed number of channels were available ($n = 4$), plasma incubated at room temperature between 45 and 60 min prior to initiation of coagulation.

The third series of experiments was designed to decrease incubation time by increasing temperature and deferoxamine concentration without compromising the ability to detect iron-mediated changes in R values. In these experiments, plasma had a 1% v/v addition of PBS or $FeCl_3$ (10 μmol/l final concentration) followed by a 3 min incubation at room temperature. Subsequently, 330 μl of either of these plasma types was placed in disposable thrombelastograph cups, with addition of dH_2O or deferoxamine (2.78 mmol/l final concentration). The mixtures were mixed with the disposable pin and allowed to incubate for 15 min at 37°C. Clotting was initiated with 20 μl of $CaCl_2$ and data were collected at 37°C until R was recorded. Six replicates of the four conditions were analyzed.

Scanning electron micrographic-based analyses

All SEM-based analyses were conducted at the University of Pretoria. For the SEM experiments, 80 ml of whole blood was collected from a single donor, and anticoagulated with sodium citrate (nine parts blood to one part 0.105 mol/l sodium citrate), and platelet-rich plasma (') was obtained from each collected sample by centrifuging the whole blood at 1250*g* for 2 min. The donor was a healthy, nonsmoking female individual (age: 45; serum ferritin level: 13 ng/ml; and percentage of iron saturation: 22%).

In the SEM experiments, six different combinations of products and incubation times were prepared. Combination 1 (C1) consisted of 1 ml of PRP mixed with 10 μl of PBS and 10 μl of double-distilled water. Combination 2 (C2) consisted of 1 ml of PRP mixed with 10 μl PBS and 10 μl of 100 mmol/l deferoxamine, followed by incubation for 3 min at room temperature. Combination 3 (C3) consisted of 1 ml PRP mixed with 10 μl of 1 mmol/l $FeCl_3$, followed by incubation at room temperature for 3 min. Combination 4 (C4) consisted of 1 ml PRP mixed with 10 μl of 1 mmol/l $FeCl_3$, followed by incubation at room temperature for 3 min; 10 μl of 100 mmol/l deferoxamine was then added. Combination 5 (C5) consisted of 1 ml PRP mixed with 10 μl of 1 mmol/l $FeCl_3$ and 10 μl

of double-distilled water. This mixture was incubated at room temperature for 1 h. Combination 6 (C6) consisted of 1 ml PRP mixed with 10 μl of 1 mmol/l $FeCl_3$, followed by incubation at room temperature for 3 min, followed by addition of 10 μl of 100 mmol/l deferoxamine. This sample was incubated for 1 h at room temperature. After the aforementioned specified incubation period, 10 μl of each combination (C1–C6) was added to 5 μl of thrombin, mixed on a glass cover slip, and then incubated at 37°C for 3 min before further SEM analysis preparation.

SEM preparation involved a washing of C1–C6 in 0.075 mol/l PBS for 20 min to remove any plasma and product residues, followed by fixing in 4% formaldehyde in for 30 min, followed by three washing steps in 0.075 mol/l PBS for 3 min to remove any residual fixative. The smears were then postfixated for 15 min with 1% osmium tetroxide (OsO_4), followed by a washing process, for 3 min in 0.075 mol/l PBS. The samples were finally dehydrated serially in 30, 50, 70, 90%, and then three times in 100% ethanol followed by drying using hexamethyldisilazane, and then mounting and coating with carbon. Once the samples had been coated, they were examined using a SEM (Zeiss ULTRA plus FEG SEM; Carl Zeiss Microscopy GmbH, Jena, Germany). The Institutional Review Board of the University of Pretoria granted approval for healthy individuals for SEM-based investigations [ethics number 151/2006 (E Pretorius) that is extended until end of 2014].

Statistical analyses and graphics

R data are presented as mean ± standard deviation, with analyses conducted with a commercially available statistical program (SigmaStat 3.1; Systat Software, Inc, San Jose, California, USA). Graphics were generated with a commercially available program (OrigenPro 7.5; OrigenLab Corporation, Northampton, Massachusetts, USA). The analysis of the effects of increasing the concentration of $FeCl_3$ on R values was conducted with one-way analysis of variance with the Holm-Sidak post-hoc test. As the subsequent data generated in thrombelastographic experiments violated assumptions of normality and variance, these analyses of the effects of $FeCl_3$ and deferoxamine on R values were conducted with Kruskal–Wallis one-way analysis of variance with the Student–Newman–Keuls post-hoc test. A P value of less than 0.05 was considered significant. Micrographs of SEM data were generated with Adobe Photoshop CS6 (Adobe Systems Inc., San Jose, California, USA).

Results

Thrombelastographic data

Data from the various series of experiments are displayed in Fig. 1 and Table 1. As seen in Fig. 1, the addition of 2–10 μmol/l $FeCl_3$ to plasma resulted in significantly smaller R values than plasma without $FeCl_3$ addition. Only samples exposed to 10 μmol/l $FeCl_3$ had R values

Fig. 1

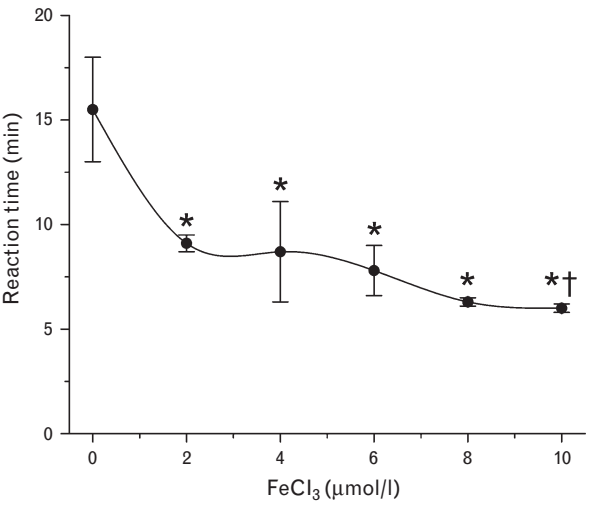

Effects of $FeCl_3$ concentration on reaction time in normal plasma. Data presented as mean ± standard deviation. *$P < 0.05$ vs. 0 μmol/l, †$P < 0.05$ vs. 2 μmol/l.

significantly smaller than those exposed to 2 μmol/l $FeCl_3$. The degree of reduction in R values by addition of $FeCl_3$ varied by 39–61% of values observed in samples not exposed to $FeCl_3$.

The results concerning the effects of chelation on R values are depicted in Table 1. Exposure to deferoxamine for 3 min resulted in a small but significant decrease in R values compared with control plasma values. Exposure to $FeCl_3$ resulted in a significant 54% reduction in R values compared with control plasma values. This significant, $FeCl_3$-mediated decrease in R values did not significantly change when deferoxamine was added for an additional 3 min incubation. However, after a 45–60 min incubation, the significant, $FeCl_3$-mediated (72%) decrease in R values was significantly attenuated by addition of deferoxamine. Compared with samples with $FeCl_3$ addition alone, samples incubated with deferoxamine for 45–60 min after $FeCl_3$ addition had a 108% increase in R values. This pattern of successful chelation of iron by deferoxamine and partial restoration of R values toward that of control plasma was observed in plasma incubated at 37°C for 15 min following addition of 2.78 mmol/l deferoxamine.

Scanning electron micrographic data

Figures 2 and 3 shows a low (40 000× machine magnification) and higher SEM magnification (100 000× machine magnification), respectively, of the fibrin fibers created with the addition of thrombin. During fibrin formation, wherein thrombin is added to PRP, a fibrin net is formed with mainly thick, major fibers (Figs 2a and 3a, white arrow). When deferoxamine is added to PRP and a net is created with thrombin, the fibers do not differ

Table 1 Effects of $FeCl_3$ and deferoxamine on reaction time (min)

Control	Deferoxamine	FeCl3	FeCl3 + deferoxamine
Three-minute incubation at room temperature, deferoxamine 1 mmol/l			
13.4 (12.7, 14.4)	11.6 (11.2, 12.1)[a]	5.9 (5.8, 6.4)[a,b]	6.2 (4.9, 6.3)[a,b]
Forty-five to 60-min incubation at room temperature, deferoxamine 1 mmol/l			
17.9 (15.2,20.4)	17.4 (16.2,18.6)	5.0 (4.9,5.1)[a,b]	10.4 (9.5,11.0)[a,b,c]
Fifteen-minute incubation at 37°C, deferoxamine 2.78 mmol/l			
18.8 (14.0, 29.1)	16.2 (13.1, 19.7)	4.6 (4.4, 6.0)[a,b]	9.2 (9.0, 9.4)[a,c]

$FeCl_3$ final concentration was 10 μmol/l in all conditions where present. Data are presented as median (1st, 3rd quartile). [a] $P < 0.05$ vs. control [b] $P < 0.05$ vs. deferoxamine [c] $P < 0.05$ vs. $FeCl_3$.

significantly visually between healthy fiber net and the addition of the iron chelator (Figs 2b and 3b).

With the addition of iron to PRP and net creation with thrombin, we have previously reported a changed fibrin fiber formation, wherein the fibers do not form individual recognizable entities. Addition of iron causes the fibers to form plates (Fig. 2c, star) and areas showing a dense fine net, and higher magnification shows the plated dense matted deposits (Fig. 3c, arrow) that individual fibers fuse longitudinally (star). Where PRP is exposed to iron followed by a 3-min deferoxamine exposure (Figs 2d

Fig. 2

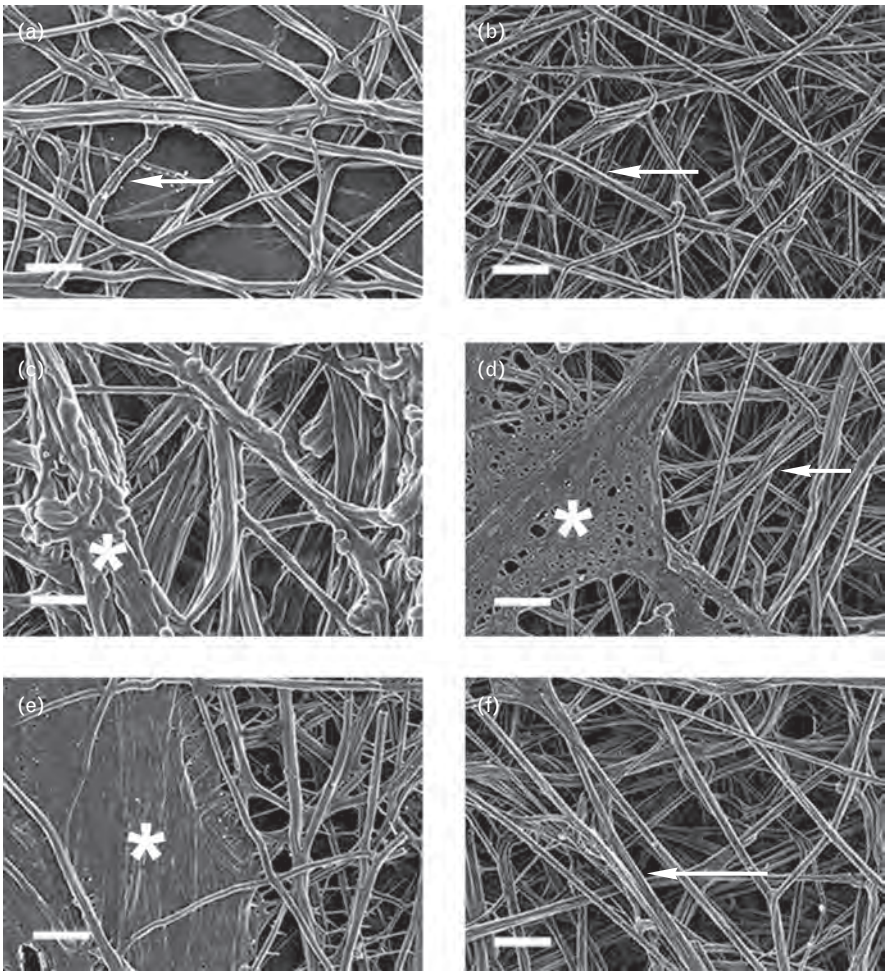

Scanning electron microphotographs of platelet-rich plasma (PRP) after exposure to $FeCl_3$ and/and deferoxamine at low magnification followed by addition of thrombin before washing and fixing in all experiments to create extensive fibrin network. (a) 1 ml PRP + 10 μl PBS + 10 μl double-distilled water (combination 1, C1); (b) 1 ml PRP + 10 μl PBS + 10 μl of a 100 mmol/l deferoxamine (C2); (c) 1 ml PRP + 10 μl of a 1 mmol/l $FeCl_3$, incubate 3 min, (C3); (d) 1 ml PRP + 10 μl of a 1 mmol/l $FeCl_3$, add 10 μl 100 mmol/l deferoxamine and incubate for 3 min (C4); (e) 1 ml PRP + 10 μl of a 1 mmol/l $FeCl_3$, incubate 3 min, incubate for 1 h at room temperature (C5); (f) 1 ml PRP + 10 μl of a 1 mmol/l $FeCl_3$; incubate 3 min, then add 10 μl of 100 mmol/l deferoxamine and incubate for 1 h at room temperature (C6). Machine magnification is 40 000× and scale = 1 μm.

Fig. 3

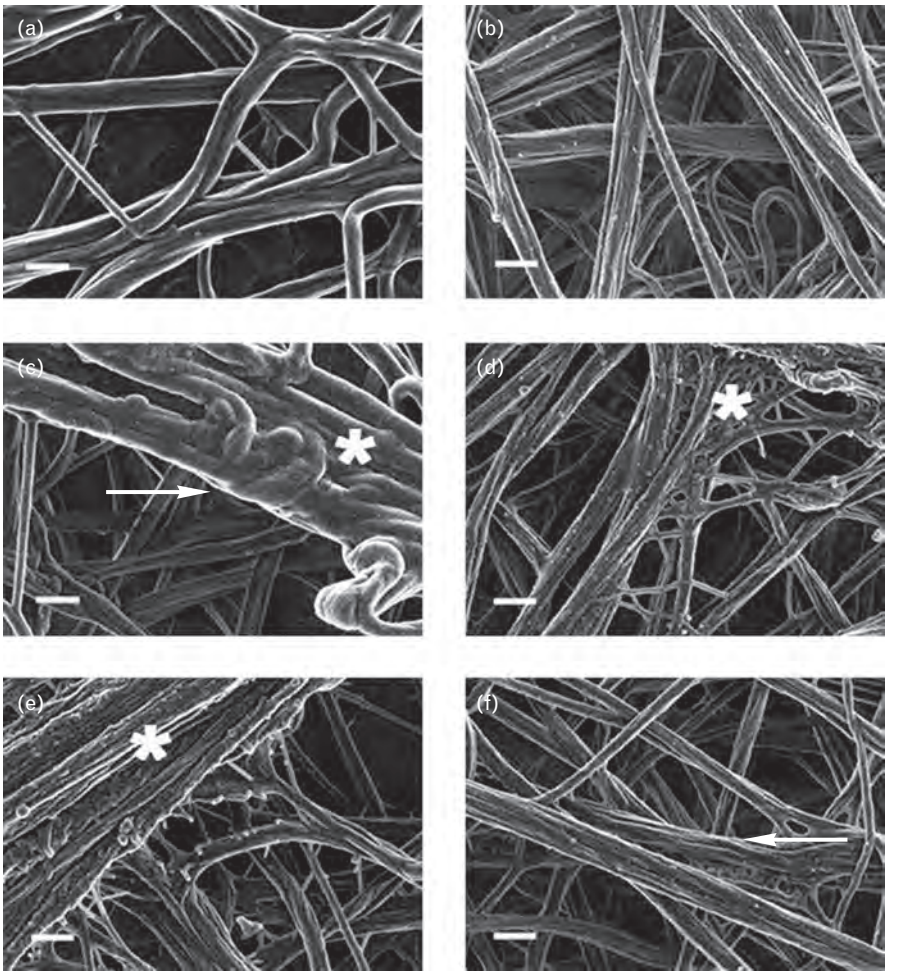

Scanning electron microphotographs of platelet-rich plasma (PRP) after exposure to $FeCl_3$ and/or deferoxamine at high magnification followed by addition of thrombin before washing and fixing in all experiments to create extensive fibrin network. (a) 1 ml PRP + 10 μl PBS + 10 μl double-distilled water (combination 1, C1); (b) 1 ml PRP + 10 μl PBS + 10 μl of a 100 mmol/l deferoxamine (C2); (c) 1 ml PRP + 10 μl of a 1 mmol/l $FeCl_3$, incubate 3 min, (C3); (d) 1 ml PRP + 10 μl of a 1 mmol/l $FeCl_3$, add 10 μl 100 mmol/l deferoxamine and incubate for 3 min (C4); (e) 1 ml PRP + 10 μl of a 1 mmol/l $FeCl_3$, incubate for 3 min, incubate for 1 h at room temperature (C5); (f) 1 ml PRP + 10 μl of a 1 mmol/l $FeCl_3$; incubate 3 min, then add 10 μl 100 mmol/l deferoxamine and incubate for 1 h at room temperature (C6). Machine magnification is 100 000× and scale = 300 nm.

and 3d), the matted plates seem to be less dense (star on both figures) and the individual fibers are no longer fused longitudinally (Fig. 3d, arrow).

We also investigated the effect of time on the fibrin formation. Figs 2e and 3e show PRP exposed to iron for 1 h followed by net creation by adding thrombin. This experiment was done at room temperature and in a capped Eppendorf tube. Prolonged iron exposure caused the fibrin fibers to form a much thicker homogenous dense matted deposit, wherein nearly no individual fibers are visible at the lower magnification (Fig. 3e, star). However, at the higher magnification (Fig. 4e, star), individual, longitudinally fused fibers can still be seen. When deferoxamine is added 3 min after the iron was added to PRP and this mixture was also left for 1 h in a capped Eppendorf tube at room temperature, before thrombin was added (Figs 2f and 3f), the fibrin nets are not as matted as without the iron chelator, and individual fibrin fibers are again visible, although not fully restored as is seen in a typical healthy fibrin fiber network (arrows).

Discussion

The primary finding of the present investigation was that the coagulation kinetic and ultrastructural changes induced by clinically encountered free iron concentrations were partially attenuated by chelation with deferoxamine. This finding is critical, as binding without generation of radical species with consequent conformational changes in fibrinogen structure can now be entertained as an important mechanism by which iron

mediates hypercoagulability. As we previously noted, radical species typically irreversibly decrease fibrinogen function in an irreversible fashion [13,14], and our experiments demonstrated reversibility secondary to iron chelation and presumed unbinding of iron from fibrinogen. The residual effects of iron after chelation may be secondary to incomplete removal of exogenously added iron or some other iron-mediated effect on fibrinogen that is not reversible, or both. The extent of return of coagulation function following chelation of plasma with 10 μmol/l $FeCl_3$ addition was equivalent to a R value similar to that associated with plasma exposed to 2 μmol/l $FeCl_3$ (compare Fig. 1 and Table 1 R values). In sum, although complete reversal of iron-mediated changes in thrombelastographic and SEM-derived data was not achieved, partial reversal with chelation strongly supports iron binding as a significant mechanism mediating hypercoagulability.

Given this new paradigm, a reexamination of both thrombophilic states associated with iron overload is indicated. Using deferoxamine-mediated chelation, appropriate temperature, and sufficient incubation time, it will be potentially possible to assess the impact of iron with thrombelastography, thromboelastimetry, or SEM. Thus, as reviewed [1], the role of ferritin and free iron excess in chronic diseases such as diabetes mellitus, rheumatoid arthritis, or perhaps cancer [19] can be assessed. Perhaps the degree of iron-specific hypercoagulability could be correlated with clinical disease, and in turn, such diagnostics could be used to assess the effectiveness of therapy targeted at diminishing circulating iron concentrations or interventions that diminish inflammatory processes that result in iron overload. The utility of such a diagnostic evaluation of iron-mediated hypercoagulability in research or clinical settings will be defined in future investigations.

In conclusion, using thrombelastographic and SEM approaches, we have determined that reversible iron binding to presumably fibrinogen is an important mechanism by which iron causes hypercoagulability. Additional study will be required to further determine whether residual binding or other iron-mediated effects are responsible for residual hypercoagulability observed after chelation.

Acknowledgements

Grant support: This investigation was supported by the Departments of Anesthesiology and Physiology.

Conflicts of interest

The authors declare no conflicts of interest.

References

1 Kell DB, Pretorius E. Serum ferritin is an important inflammatory disease marker, as it is mainly a leakage product from damaged cells. *Metallomics* 2014; **6**:748–773. doi: 10.1039/c3mt00347g.
2 Lipinski B, Pretorius E. Novel pathway of iron-induced blood coagulation: implications for diabetes mellitus and its complications. *Pol Arch Med Wewn* 2012; **122**:115–122.
3 Lipinski B, Pretorius E, Oberholzer HM, van der Spuy WJ. Iron enhances generation of fibrin fibers in human blood: implications for pathogenesis of stroke. *Microsc Res Tech* 2012; **75**:1185–1190.
4 Pretorius E, Vermeulen N, Bester J, Lipinski B. Novel use of scanning electron microscopy for detection of iron-induced morphological changes in human blood. *Microsc Res Tech* 2013; **76**:268–271.
5 Lipinski B, Pretorius E. Iron-induced fibrin in cardiovascular disease. *Curr Neurovasc Res* 2013; **10**:269–274.
6 Pretorius E, Lipinski B. Differences in morphology of fibrin clots induced with thrombin and ferric ions and its pathophysiological consequences. *Heart Lung Circ* 2013; **22**:447–449.
7 Pretorius E, Oberholzer HM, van der Spuy WJ, Swanepoel AC, Soma P. Qualitative scanning electron microscopy analysis of fibrin networks and platelet abnormalities in diabetes. *Blood Coagul Fibrinolysis* 2011; **22**:463–467.
8 Pretorius E, Oberholzer HM, van der Spuy WJ, Swanepoel AC, Soma P. Scanning electron microscopy of fibrin networks in rheumatoid arthritis: a qualitative analysis. *Rheumatol Int* 2012; **32**:1611–1615.
9 Lipinski B. Modification of fibrin structure as a possible cause of thrombolytic resistance. *J Thromb Thrombolysis* 2010; **29**:296–298.
10 Lipinski B, Pretorius E. Hydroxyl radical-modified fibrinogen as a marker of thrombosis: the role of iron. *Hematology* 2012; **17**:241–247.
11 Pretorius E, Vermeulen N, Bester J, Lipinski B, Kell DB. A novel method for assessing the role of iron and its functional chelation in fibrin fibril formation: the use of scanning electron microscopy. *Toxicol Mech Methods* 2013; **23**:352–359.
12 Pretorius E, Bester J, Vermeulen N, Lipinski B, Gericke GS, Kell DB. Profound morphological changes in the erythrocytes and fibrin networks of patients with hemochromatosis or with hyperferritinemia, and their normalization by iron chelators and other agents. *PLoS One* 2014; **9**:e85271.
13 Shacter E, Williams JA, Levine RL. Oxidative modification of fibrinogen inhibits thrombin-catalyzed clot formation. *Free Radic Biol Med* 1995; **18**:815–821.
14 Martinez M, Weisel JW, Ischiropoulos H. Functional impact of oxidative posttranslational modifications on fibrinogen and fibrin clots. *Free Radic Biol Med* 2013; **65**:411–418.
15 Yeum KJ, Russell RM, Krinsky NI, Aldini G. Biomarkers of antioxidant capacity in the hydrophilic and lipophilic compartments of human plasma. *Arch Biochem Biophys* 2004; **430**:97–103.
16 Orino K. Functional binding analysis of human fibrinogen as an iron- and heme-binding protein. *Biometals* 2013; **26**:789–794.
17 Nielsen VG, Cohen JB, Malayaman SN, Nowak M, Vosseller K. Fibrinogen is a heme-associated, carbon monoxide sensing molecule: a preliminary report. *Blood Coagul Fibrinolysis* 2011; **22**:443–447.
18 Nielsen VG, Pretorius E. Iron and carbon monoxide enhance coagulation and attenuate fibrinolysis by different mechanisms. *Blood Coagul Fibrinolysis* 2014; in press, PMID: 24732176.
19 Panis C, Victorino VJ, Herrera ACSA, Freitas LF, De Rossi T, Campos FC, *et al.* Differential oxidative status and immune characterization of the early and advanced stages of human breast cancer. *Breast Cancer Res Treat* 2012; **133**:881–888.